Proton-air cross section measurement with ARGO-YBJ

C. Bleve*† , I. De Mitri*†, L. Perrone‡†, A. Surdo†
(on behalf of the ARGO-YBJ Collaboration)

*Dipartimento di Fisica, Università del Salento, I-73100, Lecce, Italy
†Istituto Nazionale di Fisica Nucleare (INFN), Sezione di Lecce, I-73100, Lecce, Italy
‡Dipartimento di Ingegneria dell'Innovazione, Università del Salento, I-73100, Lecce, Italy

Abstract. **The proton-air cross section in the energy range 1-100 TeV has been measured with the ARGO-YBJ experiment. The effects of shower fluctuations, the contribution of heavier primaries and the uncertainties of the hadronic interaction models, have been taken into account. The results have been used to estimate the total proton-proton cross section at center of mass energies between 70 and 500 GeV, where no accelerator data are currently available.**

Keywords**: Cross Section, Hadronic Interactions, Extensive Air Showers**

I. INTRODUCTION

The p-air cross section is measured with cosmic ray (CR) experiments by evaluating the absorption of the primary proton flux penetrating the atmosphere [1]. In this paper we will report on the measurement of the *production* cross section [2], hereafter simply σ_{p-air}, between 1-100 TeV CR protons and *"air"* nuclei with the ARGO-YBJ experiment. Details can be found in [3].

The ARGO-YBJ detector is a full coverage extensive air shower array made by a single layer of Resistive Plate Chambers (RPCs) operated in streamer mode, providing a time resolution at the nanosecond level. The array is organized in 153 clusters of 12 RPCs. Each RPC is read out by ten $62 \times 56\,\mathrm{cm}^2$ pads, which are further divided into 8 strips, thus providing a larger particle counting dynamic range [4], [5], [6]. The array is located in the village of YanBaJing (Tibet,China) at an altitude of 4300 m above sea level (corresponding to a vertical atmospheric depth of about $610\,\mathrm{g/cm}^2$) and it is in smooth data taking from mid 2006.

For a primary energy interval and for a given distance (grammage) X_{dm} between the detector and the shower maximum, the frequency of showers as a function of zenith angle θ is directly related to the probability distribution of the depth of the shower maximum $P(X_{max})$, where $X_{max} = h_0 sec\theta - X_{dm}$ and h_0 is the observation vertical depth. The shape of $P(X_{max})$ is given by the folding of the exponential dependence of the depth of the first interaction point X_0 (i.e. $e^{-X_0/\lambda_{p-air}}$ with $\lambda_{p-air}(g/cm^2) \simeq 2.41 \times 10^4/\sigma_{p-air}(mb)$), with the probability distribution of $X_{rise} \equiv X_{max} - X_0$, which includes the fluctuations of the shower development up to its maximum. Then the effects of the limited experimental resolution have to be also taken into account. For sufficiently large X_{max} values, $P(X_{max})$ tends to be a simple exponential with a characteristic length $\Lambda = k\lambda_{p-air}$, where k depends on hadronic interactions and on the shower development in the atmosphere and its fluctuations [7]. The actual value of k must be evaluated with a full Monte Carlo (MC) simulation and it depends on the experimental approach, the primary energy and the detector response. Finally, the contribution of cosmic rays heavier than protons has to be estimated and minimized in order to get an unbiased proton-air cross section measurement.

Experiments using the air fluorescence technique have direct access to $P(X_{max})$, while EAS detectors measuring the particles at ground might sample it through the flux dependence on zenith angle, once X_{dm} (or the shower age) has been fixed or constrained, within the limits of detector capabilities. In these cases the combination of CR energy, detector vertical depth, angular and X_{dm} ranges, actually define the part of the X_{max} distribution that can be accessed. A good performance is obtained if the exponential tail of $P(X_{max})$ can be sampled. This requires selecting showers with the maximum development not far from the detection level (i.e. minimizing X_{dm}) and, obviously, exploring a zenith angle region as wide as possible. If this is not the case, a flattening of the distribution might be observed, also due to shower fluctuations, resulting in a larger value of the parameter k and a lower sensitivity to σ_{p-air}.

The ARGO-YBJ detector features and location (full coverage, angular resolution, fine granularity, small atmospheric depth, etc.), which ensure the capability of reconstructing the detected showers in a very detailed way, have been used to define the energy ranges and to constrain the shower ages. In particular, different hit (i.e. strip) multiplicity windows have been used to select showers corresponding to different primary energies, while the information on particle density, lateral profile and shower front extension has been used to constrain X_{dm} in the proper range. These features allowed the observation of the exponential falling of shower frequencies, through the $sec\theta$ distribution

The fit to the angular distribution $R(\theta)$ gives the slope value α, connected to the observed characteristic length Λ through the relation $\alpha = h_0/\Lambda$, being

$$R(\theta) = A(\theta)\, R_0\, e^{-\alpha(sec\theta - 1)} \qquad (1)$$

where R_0 = $R(\theta$=0), and the factor $A(\theta)$ takes into

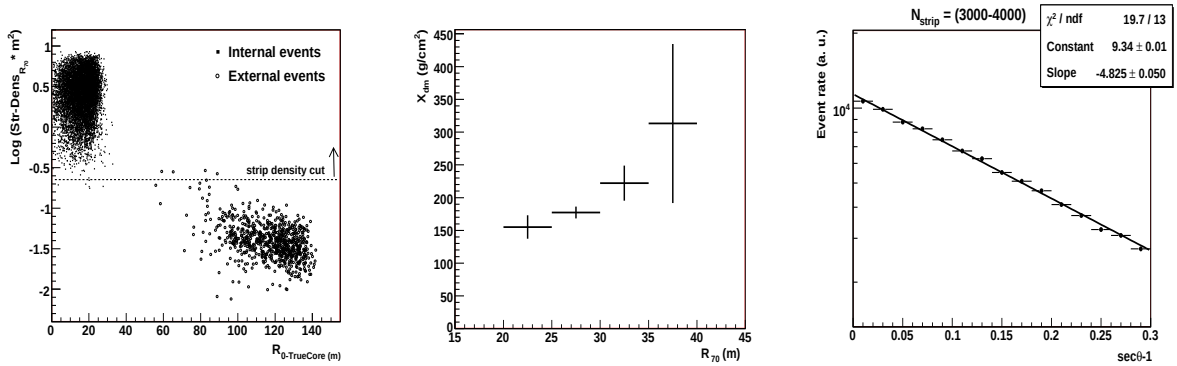

Fig. 1. LEFT: Correlation between the strip density near the reconstructed core and distance of the true shower core from the detector center. As can be seen, the *density cut* (dashed line) is able to efficiently reject misreconstructed events. CENTER: Correlation between R_{70} and X_{dm}. The cut $R_{70} \leq 30\,\mathrm{m}$ allows the selection of events with small X_{dm} (i.e. deeper shower maximum). The plots shown in the left and center panels refer to simulated proton-induced showers processed as real data. RIGHT: Experimental $sec\theta$ distributions for one of the five strip multiplicity ranges, after correction for the geometrical acceptance in each angular bin.

account the geometrical acceptance of each angular bin.

The same analysis chain is then applied to the simulated data sample (see next section). For each strip multiplicity (i.e. primary energy) interval, the fit to the $sec\theta$ distribution with the function of Eq.1 gives the value of Λ^{MC}. The value of k, referring to each multiplicity bin, can then be evaluated as $k = \Lambda^{MC}/\lambda^{MC}_{p-air}$, where λ^{MC}_{p-air} is known, in the corresponding energy region, from the adopted interaction model.

The experimental interaction length is obtained by correcting the observed characteristic length Λ^{exp}_{CR-air} by the factor k determined on the basis of the MC simulation: $\lambda^{exp}_{CR-air} = \Lambda^{exp}_{CR-air}/k$. Such value will give the measured p-air interaction length (λ^{exp}_{p-air}), once the effects of heavier nuclei present in the primary cosmic ray flux have been taken into account (see Sec.III).

The proton-air *production* cross section is then obtained from the previously mentioned relation: $\sigma_{p-air}\,(\mathrm{mb}) = 2.41 \times 10^4/\lambda^{exp}_{p-air}\,(\mathrm{g/cm^2})$, while theoretical models based on the Glauber theory [9] can be applied to get the corresponding total proton-proton cross section σ_{p-p}, as discussed in several works [7].

II. Data Selection and Monte Carlo simulation

The analysis was applied to a data sample of about 6.5×10^8 events collected by the central part of the detector, i.e. the 130 adjoining clusters, fully covering a surface of $78 \times 74\,\mathrm{m^2}$. In order to have both a small contamination of *external* events (i.e. those events with the true core position outside the carpet but reconstructed inside) and an angular resolution better than 0.5°, only events with at least 500 fired strips were considered. Moreover, the analysis was restricted to events with reconstructed zenith angle $\theta \leq 40°$. This was made in order to avoid effects due to the possible zenith angle dependence of the analysis cuts, that might occur at $\theta \gtrsim 45°$ (see below).

A full simulation chain was also set up to check the effects of the different analysis cuts and to estimate possible systematics. About 10^8 proton-initiated and 2×10^7 He-initiated showers, with the corresponding power law energy spectra between 300 GeV and 3000 TeV and zenith angle up to 45°, were produced with *CORSIKA* [10]. In order to have a better evaluation of systematics, we produced independent samples by using three different hadronic interaction models: *QGSJET-I* [11], *QGSJET-II.03* [12], and *SIBYLL-2.1* [13].

After a first event selection based on the quality of the reconstruction procedure, a further rejection of *external* showers was performed with several additional cuts listed in the following. The reconstructed core position, P_{rc}, was required to be in a fiducial area given by the inner 11×8 RPC clusters (a total surface of about $64\times64\,\mathrm{m^2}$). The quantity R_{70} was then introduced as the radius of the smallest circle (lying on the detector plane and centered in P_{rc}) containing 70% of the fired strips. It was then required that the distance of P_{rc} from the detector center plus R_{70} should be less than 50 m. The aim of this cut was to select showers largely contained inside the detector area (thus very well reconstructed). One further cut required the minimum average fired strip density, within a distance R_{70} from the reconstructed core, to be $0.2\,\mathrm{strips/m^2}$ in the shower plane. This *density cut* allowed the efficient rejection of *external* events, as shown in Fig. 1, left panel. The same purpose motivated the last selection cut (a *compactness cut*), requiring the R_{70} radius to be at most 30 m. Monte Carlo simulations showed that this *compactness cut* is also related to the shower development stage, allowing the constraint of the value of X_{dm} (Fig. 1, central panel) and the selection of showers with their maximum lying deep in the atmosphere (i.e. the sampling of the exponential tail of the X_{max} distribution). The last two cuts finally selected 12% of the events reconstructed with $\theta \leq 40°$ and $N_{strip} \geq 500$ in the initial data sample. The fractions of events surviving each analysis cut were checked to be consistent with the corresponding quantities for MC data. The selected data sample was split into five different bins of strip multiplicity ΔN_{strip}, starting from the threshold value of 500 fired strips on

the whole central detector (out of the total 124800), in the trigger time window of 420 ns. As shown in Tab.I, each strip multiplicity bin corresponds to a different primary energy interval. The distributions of primary energies and X_{dm} of simulated events surviving the analysis selection were also checked to be independent of the zenith angle up to about 40°, thus showing that the experimental sensitivity is not compromised by shower-to-shower fluctuations [14], [15].

III. Results and discussion

In Fig.1 (right panel), the experimental $sec\theta$ distribution for one of the five strip multiplicity ranges is shown. In all the multiplicity windows, the distributions follow the expected exponential behaviour, this being a further check that the detector capabilities and the adopted analysis cuts brought to a proper selection of events for the cross section measurement. A slight deviation is present, for the lowest energy sample only, at small $sec\theta$ values (therefore not included in the fit). This is interpreted as due to the effect of shower fluctuations, the shower maximum being more distant from the detector for these events. Indeed, for the lowest energy sample $\langle X_{max} \rangle \simeq 390\,\mathrm{g/cm^2}$, while $\langle X_{max} \rangle \simeq 450\,\mathrm{g/cm^2}$ for the other ones.

The $sec\theta$ distributions obtained from the MC simulations are very similar to those obtained with real data and the same considerations can be applied. From these plots, the values of Λ^{MC} are extracted. Once divided by the values of λ^{MC}_{p-air}, they give the parameter k for the different energies. As mentioned before, we produced three independent MC samples with different hadronic interaction models, namely *QGSJET-I*, *QGSJET-II.03*, and *SIBYLL-2.1*. In the 1-100 TeV primary energy range, their predictions for σ_{p-air} are quite similar, while there are larger differences for the estimates of the rate of diffraction processes and for the inelasticity of proton air interactions [16]. The k factors were evaluated separately with *QGSJET-I*, *QGSJET-II.03* and *SIBYLL-2.1*. In order to have a comprehensive and conservative approach, we decided to consider all of them in the current analysis and to take the spread among different models (at the level of few per cent) as a further source of systematic error (see tab.I). As can be seen, in our case $k \simeq 1.6 \div 1.8$, apart from the values obtained at the boundaries of the covered energy region. The larger value of k for the lowest energy bin is due to the smaller $\langle X_{max} \rangle$ value, that produces a larger effect of shower-to-shower fluctuations (see Sec.I). An explanation for the relatively high value of k in the highest energy bin is given by the onset of saturation of the strip digital information used in the analysis. This makes wider the energy interval actually contributing to the considered multiplicity bin, therefore implying a larger effect of fluctuations, mainly in terms of X_{rise}, with a consequent loss of sensitivity. These two effects practically define the energy region in which the current analysis can be performed.

As outlined in Sec.I, the measured Λ^{exp}_{CR-air} value together with the k factor determined from the simulation, directly gives the experimental interaction length λ^{exp}_{CR-air} and consequently the production cross section σ_{CR-air}. At this stage, the cross section has still to be corrected for the contribution of CR primaries heavier than protons. This correction has been estimated by evaluating the effect of the introduction of helium primaries in the simulated data on the shape of the $sec\theta$ distribution, for each multiplicity interval. Corrections for other primaries (i.e. CNO group, Fe, etc.) are negligible. The proton and helium fluxes reported in [17] were considered as reference values, while the systematic effect due to the uncertainty of the primary CR composition has been estimated by applying the same procedure starting from the JACEE[18] and RUNJOB[19] measurements. The slope of the $sec\theta$ distribution changed at most by 5%. This has been checked to be due not only to the CR beam composition itself, but also because the analysis cuts actually select a proton-enriched sample. After these corrections, the resulting proton-air production cross sections, σ_{p-air}, are summarized in Tab.I, where both statistical and systematic errors are reported. These values are consistent with a previous ARGO-YBJ measurement done without using the strip information [20], and also with a preliminary estimate obtained from the analysis of a data set taken with only 42 RPC clusters during the detector installation [21], [22].

The measured p-air *production* cross section is also reported, in Fig.2, as a function of the primary proton energy, together with the results found by other experiments and the expectations given by some hadronic interaction models. As can be seen latest results, namely those from ARGO-YBJ, EAS-TOP and HiRes [1], systematically give cross section values that are slightly lower with respect to the more recent and comprehensive hadronic interaction models actually used in these analyses. The indication for lower cross section (and/or inelasticity) values is also consistent with what found from the analysis of several other EAS observables [1], [23], [24]. Residual systematic differences between data and expectations at the level of few per cent might also result from the modeling and the effect of very low inelasticity collisions. This kind of effects might be different in the case of cross section evaluations based on measurements of the single hadrons flux at ground [1]. The low energy threshold of ARGO-YBJ (with respect to other EAS experiments) allows a direct comparison with the values given by this technique, showing a good agreement. This is particularly important since the systematics of the two measurement techniques are completely different. The agreement also extends to the predictions of different calculations based on the Glauber theory [9], applied to the measurements made at particle accelerators. As an example, the results of two of them [25], [26] are actually shown in Fig.2, starting from the accelerator data analysis performed in [27].

As outlined in Sec.I, the Glauber theory can also

ΔN_{strip}	Log(E/eV)	k	σ_{p-air} (mb)	σ_{p-p} (mb)
$500 \div 1000$	12.6 ± 0.3	$1.93 \pm 0.05 \pm 0.06$	$272 \pm 13 \pm 9$	$43 \pm 3 \pm 5$
$1500 \div 2000$	13.0 ± 0.2	$1.63 \pm 0.03 \pm 0.08$	$295 \pm 10 \pm 14$	$48 \pm 3 \pm 6$
$3000 \div 4000$	13.3 ± 0.2	$1.70 \pm 0.03 \pm 0.04$	$318 \pm 15 \pm 8$	$54 \pm 4 \pm 6$
$5000 \div 8000$	13.6 ± 0.2	$1.84 \pm 0.03 \pm 0.10$	$322 \pm 15 \pm 20$	$56 \pm 4 \pm 7$
> 8000	13.9 ± 0.3	$2.03 \pm 0.04 \pm 0.10$	$318 \pm 15 \pm 21$	$54 \pm 4 \pm 8$

TABLE I

STRIP MULTIPLICITY INTERVALS, CORRESPONDING PROTON PRIMARY ENERGIES (AND RMS), k FACTORS, AND RESULTING CROSS SECTIONS AFTER THE CORRECTION FOR THE EFFECT OF HEAVIER PRIMARIES. THE FIRST REPORTED UNCERTAINTIES COME FROM STATISTIC, THE SECOND ONES FROM SYSTEMATICS.

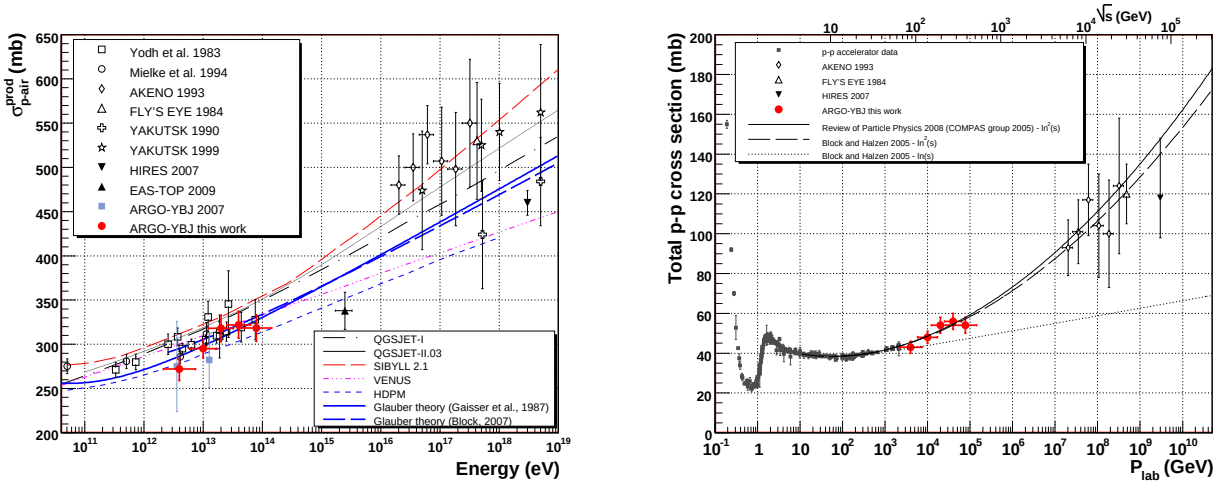

Fig. 2. Proton-air *production* and total p-p cross sections as a function of energy (see text).

be used to estimate the total proton-proton cross section σ_{p-p}, starting from σ_{p-air} as measured by CR experiments. An essential step in the conversion is the knowledge of the dependence of the slope, B, of the forward scattering amplitude for elastic p-p collisions on the center of mass energy $\sqrt{s}$, or on σ_{p-p} itself. For ARGO-YBJ data, we applied the conversion given in [25], that uses the somewhat model-independent Chou-Yang prescription [28] between B and the total cross section σ_{p-p}, this being also consistent with available measurements on $B(s)$. The results were compared with what given by several other models [7]. In all the cases the differences, in our energy range, are below 10% and they have been added as a further contribution to the systematic error on the resulting σ_{p-p}. The results are summarized in Tab.I and in Fig.2. As can be seen, the ARGO-YBJ data lie in an energy region not yet reached by p-p colliders (and still unexplored by p-$\bar{\text{p}}$ experiments [29]), favouring the asymptotic $ln^2(s)$ increase of total hadronic cross sections as obtained in [27] from a global analysis of accelerator data.

Further improvements in the analysis are expected from the use of the detailed information on the shower front (curvature, rise time, time width, etc.) that ARGO-YBJ is able to record with very high precision, and by the implementation of the analog RPC readout that will allow extending these studies to collisions with center-of-mass energies up to the TeV region.

REFERENCES

[1] J.R. Hörandel, J. of Phys. G: Nucl. Part. Phys.**29** (2003) 2439 and references therein; M. Aglietta et al., Phys. Rev. **D79** (2009) 032004; K. Belov et al., Proc. of 30th International Cosmic Ray Conference (ICRC 07), Universidad Nacional Autonoma de Mexico, Mexico City, Mexico (2008) ID 1216, Vol. 4 (HE part 1), pages 687-690
[2] R. Engel et al., Phys. Rev. **D58** (1998) 014019
[3] G.Aielli et al., (the ARGO-YBJ coll.), arXiv:0904.4198 (2009)
[4] C. Bacci et al., Astropart. Phys. **17** (2002) 151
[5] I. De Mitri et al., Nucl. Phys. **B** (Proc. Suppl.) **165** (2007) 66
[6] G. Aielli et al., Nucl. Instr. and Meth. **A562** (2006) 92
[7] M.M. Block, Phys. Rep. **436** (2006) 71, and references therein
[8] R.Ulrich et al., arXiv:0903.0404 (2009)
[9] R.J. Glauber, in *"Lectures in Theoretical Physics"*,Interscience, New York (1959);R.J. Glauber and G. Matthiae, Nucl. Phys. **B21** (1970) 135
[10] D. Heck et al. *CORSIKA: A Monte Carlo Code to Simulate Extensive Air Showers*, Forshungszentrum Karlsruhe, FZKA 6019 (1998) and references therein
[11] N. N. Kalmykov et al., Nucl. Phys. **B** (Proc. Suppl.) **52** (1997)
[12] S. Ostapchenko, Nucl. Phys. **B** (Proc. Suppl.) **151**, 143 (2006)
[13] R. Engel et al., Proc. of 26th International Cosmic Ray Conference (ICRC99), Salt Lake City, USA, (1999) vol.1, pag. 415
[14] J. Alvarez-Muniz et al., Phys. Rev. **D66** (2002) 123004
[15] J. Alvarez-Muniz et al., Phys. Rev. **D69** (2004) 103003
[16] S.Ostapchenko, Nucl. Phys. **B** (Proc. Suppl.) **175** (2008) 73
[17] J.R. Hörandel, Astropart. Phys., **19** (2003) 193
[18] K. Asakimori et al., Astrophys. J. **502** (1998) 278
[19] A.V. Apanasenko et al., Astropart. Phys. **16** (2001) 13
[20] I. De Mitri et al., Proc. of 30th International Cosmic Ray Conference (ICRC07), Universidad Nacional Autonoma de Mexico, Mexico City, Mexico (2008) ID 950, Vol. 4 (HE part 1), pages 675-678
[21] M. Iacovacci et al., Proceedings of ISVHECRI 2006, Nucl. Phys. **B** (Proc. suppl.) **175** (2008) 389
[22] A. Surdo et al., Proceedings of the 20th European Cosmic Ray Symposium, Lisbon, Portugal (2006)
[23] A.D. Erlykin, Astropart. Phys. **27** (2007) 521
[24] J. Abdallah et al., Astropart. Phys. **28** (2007) 273
[25] T.K. Gaisser et al., Phys. Rev. **D36** (1987) 1350
[26] M.M. Block, Phys. Rev. **D76** (2007) 111503
[27] M.M. Block and F.Halzen, Phys. Rev. **D72** (2005) 036006
[28] T.T. Chou and C.N. Yang, Phys. Lett. **B128** (1983) 457
[29] C. Amsler et al., Phys. Lett. **B667** (2008) 1